Frequency Dependence of Polarization of Pulsar CP 0328

Abstract. *The circularly polarized emission from the pulsar CP 0328 has an approximately flat spectrum in the 1-megahertz band centered at 113.6 megahertz, whereas the linearly polarized emission varies with frequency and from pulse to pulse. A simple model for the source that has a constant Faraday rotation measure fits some of the linearly polarized spectra observed for individual pulses, but changes in the rotation measure of as much as 30 radians per square meter are required between adjacent pulses. The simple model does not fit the average spectrum of the linearly polarized emission, although the average spectrum had the same form on two nights.*

The observation (*1*) of linear polarization in pulsars led to the possibility of measuring Faraday rotation toward sources where the integrated electron density is known, and thus of obtaining the average magnetic field strength along the path to the source. Subsequently, Smith (*2*) set an upper limit of 2×10^{-7} gauss for the average magnetic field strength toward the pulsar CP 0950. His method requires the amplitude and polarization of the pulses at several frequencies to be fairly constant with time so that minima caused by the changing Faraday rotation of the ionosphere could be identified. We describe here an attempt to observe Faraday rotation toward a pulsar by a method which, in principle, might measure the rotation for a single pulse.

We have observed the pulsar CP 0328 (*3*) with the 91-m transit telescope at the National Radio Astronomy Observatory and a six-channel receiver which fed a six-channel chart recorder having a time resolution of 10 msec. The receiver channels had a bandwidth of 100 khz and were spaced 200 khz apart. The center of the filter bank had a frequency of 113.55 Mhz. The telescope was equipped with two feed systems, one pointed east of the meridian having circular polarization and the other pointed west of the meridian having linear polarization. Two

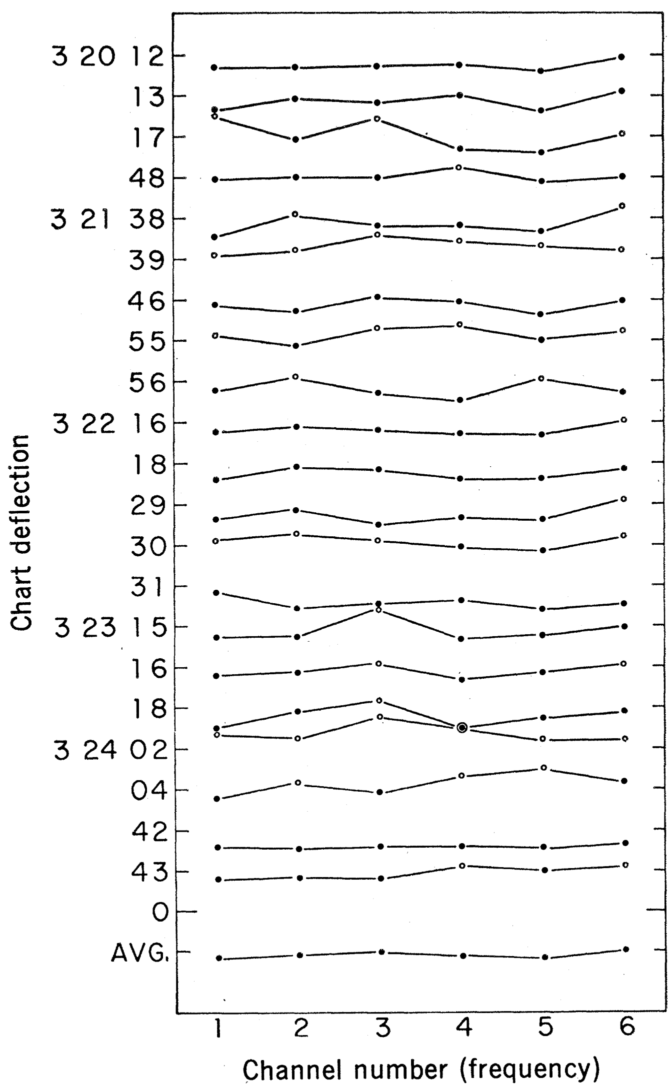

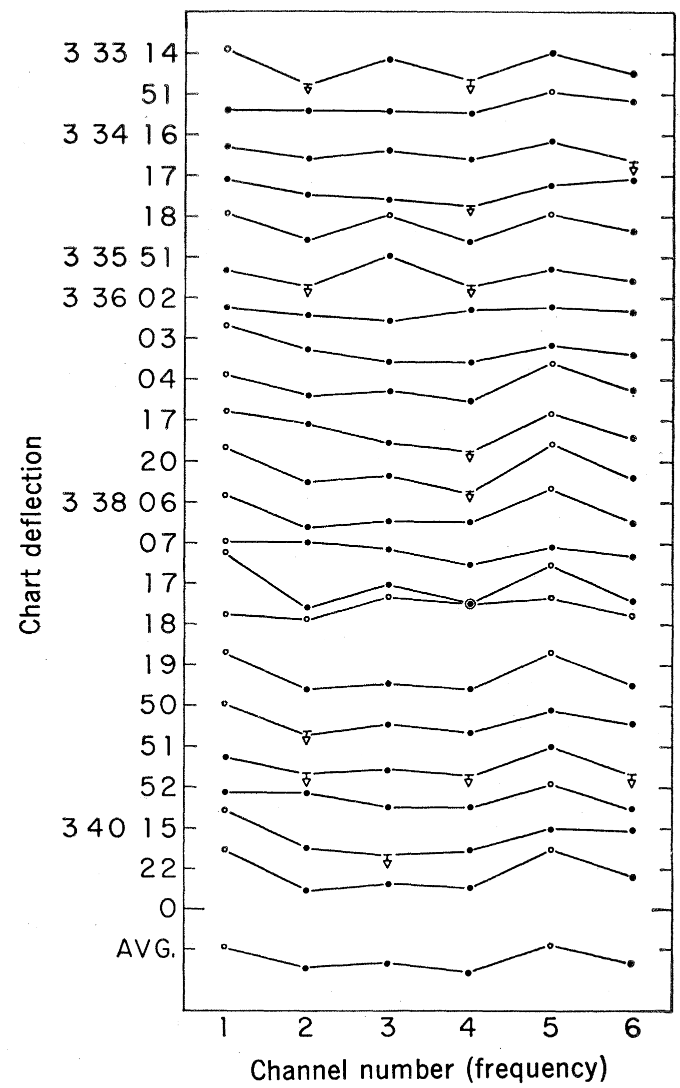

Fig. 1 (left). Peak amplitude of 21 pulses observed with circular polarization plotted against channel number. The channel numbers are arranged in order of frequency with a spacing of 200 khz. Chart deflections are shown along the ordinate; each vertical division is approximately 400×10^{-26} watt m^{-2} hz^{-1}. Open circles represent points with flux greater than one vertical division (approximately 400 flux units). The root-mean-square noise fluctuations are about one-tenth of a vertical division. The individual pulses are identified by the sidereal time to the nearest second. Fig. 2 (right). Peak amplitude of 21 pulses observed with linear polarization plotted against frequency. The vertical arrows are upper limits.

observing periods, each 11 minutes long, were successively available each night during which the effective area of the antenna was more than one-half of its maximum value.

The periodic nature of the pulsar signals was only occasionally evident on our records because few of the pulses were strong enough for easy recognition and the strong ones were not necessarily grouped. However, strong pulses were present in most of the frequency bands, and the dispersion in the arrival time (0.15-second difference between the outermost channels) was always evident.

From observations on 1 October 1968 we have selected the 21 strongest pulses observed with circular polarization and the 21 strongest pulses observed with linear polarization; the peak flux densities are plotted in Figs. 1 and 2, respectively. The curve at the bottom of each figure gives the average value of the curves plotted above. Tests with a noise source show that the variation in gain among the channels does not exceed 10 percent.

Each of the two averaged spectra agrees with the corresponding averaged spectrum obtained on another night, and they are significantly different from each other. The circularly polarized spectra are fairly uniform over the frequency band that we observed, a finding that agrees with circularly polarized observations of CP 1919 and CP 1132 (*4*). The linearly polarized spectra show variation with frequency and variation from pulse to pulse.

If the linearly polarized power and its intrinsic angle of polarization were constant over the observed frequency range and if any unpolarized or circularly polarized component were also independent of frequency, we would observe fringes in the spectrum obtained with a linearly polarized antenna, since Faraday rotation along the line of sight causes the polarization angle of the received waves to change with frequency relative to the polarization angle of the antenna (*5*). If a single value of rotation measure R applies to the whole source, the spectrum of the flux observed with a linearly polarized antenna is

$$S = S_u/2 + S_p \cos^2(R\, c^2/f^2 + \Delta\Theta) \quad (1)$$

where S_u is the unpolarized or circularly polarized flux, S_p is the linearly polarized flux, c is the velocity of light, f is the observed frequency, and $\Delta\Theta$ is the angle between the angle of intrinsic polarization of the source and that of the antenna. The spacing between maxima in the spectrum is approximately

$$\Delta f = (\pi/2)(f^3/c^2 R) \quad (2)$$

According to the Nyquist sampling criterion (*6*), the minimum value of Δf which our choice of filter spacings allows to be recognized is 400 khz. If we assume that a half cycle of a sine wave would be recognizable, the maximum value is 2000 khz. The corresponding range of rotation measures is 64.0 to 12.8 rad/m^2. The present data do not allow a unique determination of the rotation measure for several reasons. (i) Rotation measures above 64.0 rad/m^2 also produce values of Δf between 400 and 2000 khz. However, the finite width of the filters reduces the percentage of modulation for rotation measures that approach or exceed the value which puts an entire cycle in one filter. For example, rotation measures of 163 and 205 rad/m^2 give maximum percentages of modulation of 50 percent and 25 percent, respectively. (ii) Positive and negative rotation measures are indistinguishable from their spectra. (iii) A flat spectrum can indicate a rotation measure that is too high or too low to be measured with the present filter bank or a source that does not have linear polarization. A flat spectrum can also be caused by certain critical rotation measures near 64.0 rad/m^2 or an integral multiple thereof.

A curve of the form of Eq. 1 cannot be fitted satisfactorily to the average spectrum of our linearly polarized observations of CP 0328. Individual spectra (Fig. 2) in a third of the cases can be well fitted by Eq. 1, but many of the remainder cannot. Models with two or more values of R could fit all these spectra, but the limited nature of the present observations does not seem to justify considering such models here.

We consider the spectra of two adjacent pulses (Fig. 2) that can be fitted by Eq. 1, those whose sidereal times are $3^h\, 34^m\, 17^s$ and $3^h\, 34^m\, 18^s$ (the actual time difference between them is one period or 0.72 second). We assume that S_u, S_p, and $\Delta\Theta$ are all independent of frequency. The fitting of Eq. 1 gives values of R equal to 24 and 55 rad/m^2, respectively. The relation for the rotation measure in radians per square meter (*7*) is

$$R = 8.1 \times 10^5 \int n\, B\, dl \quad (3)$$

where the electron density along the path n is in electrons per cubic centimeter; the component along the line of sight of the magnetic field strength B is in gauss; and the element of path length dl is in parsecs. From our determination of the dispersion (*8*) we obtain

$$\int n\, dl = 28 \quad (4)$$

The ratio of the two integrals gives the average field strength weighted by electron density to the source of 1.0×10^{-6} gauss in the first case and 2.4×10^{-6} gauss in the second. Other values of R which also fit these spectra have larger differences.

Such rapid changes in rotation measure can only occur in or near the source (*9*); therefore, the use of the pulsar signals to determine the large-scale galactic magnetic field must await evaluation of the variable Faraday rotation within the source. The fact that many individual spectra (Fig. 2) cannot be fitted by Eq. 1 suggests that the Faraday rotation may vary with time during a single pulse. An alternate explanation is that two or more Faraday rotations may exist in different directions (or in the same direction) toward the source and that at least one Faraday rotation varies with time.

Note added in proof: Smith (*10*) has obtained a rotation measure of −95 rad/m^2 for CP 0328 from observations, each 2 minutes long, near 408 Mhz which gave the difference in power between two bands 3 and 1.5 Mhz apart while a linearly polarized feed system was rotated. His reduction was based on only part of each pulse because "it is necessary to separate out the first half of the pulse for a sufficiently large polarization to be recorded." A value of −99.4 rad/m^2 fits the linearly polarized spectra (Fig. 2) with sidereal time of $3^h\, 40^m\, 15^s$; however, if half of the pulses were unpolarized, we would not have observed any of the upper-limit points in Fig. 2. We conclude that Smith has probably not evaluated the time variation in the Faraday rotation toward CP 0328.

S. J. Goldstein, Jr.
D. D. Meisel

Department of Astronomy, University of Virginia, Box 3818, Charlottesville 22903

References and Notes

1. A. G. Lyne and F. G. Smith, *Nature* **218**, 124 (1968).
2. F. G. Smith, *ibid.*, p. 325.
3. T. W. Cole and J. D. H. Pilkington, *ibid.* **219**, 574 (1968).
4. R. M. Goldstein, *Science* **161**, 44 (1968).
5. Faraday fringes in the decameter radiation

from Jupiter have been observed by J. W. Warwick and G. A. Dulk [*Science* **145**, 380 (1964)].
6. The effect of the sampling frequency on the apparent frequency of a sine wave is discussed by R. B. Blackman and J. W. Tukey [*The Measurement of Power Spectra* (Dover, New York, 1968), p. 31].
7. F. F. Gardner and J. B. Whiteoak, *Nature* **197**, 1162 (1963).
8. Our value for the integrated electron density, 28 parsec cm^{-3}, is in good agreement with the value of 26.8 parsec cm^{-3} reported by A. G. Lyne and B. J. Rickett [*Nature* **219**, 1339 (1968)].
9. The rotation measure for the path from Earth to Jupiter had a maximum value of 0.7 rad/m^2 according to our reduction of the observations of Warwick and Dulk (*5*). Thus, even if we allow for a fourfold increase with the solar cycle, the contribution of the ionosphere to our measurements is negligible.
10. F. G. Smith, *Nature* **220**, 891 (1968).
11. We are indebted to the staff of the National Radio Astronomy Observatory for the opportunity to make these observations. The National Radio Astronomy Observatory is operated by Associated Universities, Inc., under contract with the NSF. We thank the Computer Science Center of the University of Virginia for a grant for computer time. Supported by NSF grant GP 7803.

30 October 1968; revised 19 December 1968

Sedimentary Phosphate Method for Estimating Paleosalinities: Limited Applicability

Abstract. *The sedimentary phosphate method for estimating paleosalinities was tested on argillaceous sediments from different formations and environments. Results reveal that the method cannot be used generally.*

A new method (*1*) for estimating paleosalinities in argillaceous sediments, the sedimentary phosphate method, is based on the fact that sediments act as a phosphorus reservoir in natural systems, the mineral or chemical composition of the phosphorus compounds being different in different environments. The Al-phosphate variscite and the Fe-phosphate strengite reportedly prevail in soils and fine-grained freshwater sediments, whereas the Ca-phosphate apatite is the phosphate of marine muds (*1*).

In Recent sediments from the Rappahannock River estuary, a tributary of Chesapeake Bay, a systematic change of the Fe- and Ca-phosphate proportions with increasing salinity was observed (*1*). Here the calcium to iron + calcium molar ratio increases from about 0.20 at a salinity of 1.5 per mille to 1.00 at 36 per mille and can be used as a sensitive salinity indicator over the observed salinity range.

Nelson (*1*) applied the sedimentary phosphate method to Paleozoic shales and clays from Ohio and Pennsylvania, and concluded that "the results are consistent with previous stratigraphic and fossil evidence."

We tested the new method with argillaceous muds and mudstones of Recent, Pleistocene, Tertiary, Permian, and Carboniferous ages derived from different depositional basins ranging from freshwater to hypersaline (salt clays) environment (Table 1).

The results obtained by the sedimentary phosphate method in most cases do not agree with the salinities observed directly (Recent muds, varved sediments, and Pleistocene moraines) or derived from geological or paleontological evidence.

Sediments which are nonmarine (Recent lake deposits, varved sediments, moraines, Lower Permian siltstones, and some claystones of the Upper Carboniferous) were almost marine to fully marine by the sedimentary phosphate method.

The failure of the method may be due to: (i) The materials tested may not have been exposed to weathering. The bulk minerals of Lake Constance muds and of the suspended load of its main influent, the Rhine, are not derived from soils but directly from older (mostly marine!) sediments or igneous or metamorphic rocks (containing apatite!). The same is true for the glacial sediments and most of the siltstones of the Lower Permian, the latter having been formed in an arid climate. The mineral particles were transported into the depositional basins before soil formation had taken place and, after deposition, were covered so quickly by younger sediments that no

Table 1. Salinities and paleosalinities determined by the sedimentary phosphate method (SPM) versus those obtained by direct, geological, or paleontological evidence.

Number of samples	Nature of sediment*	Salinity By SPM (‰)	Salinity Direct (‰)
	Recent		
2	Gulf of Naples; muds from pyroclastic material	35	35
3	North Sea, south of Helgoland; muds from glacial outwash	35	35
3	Lake Constance; muds, detritus from Alps via Rhine River	35	0
2	Rhine River; suspended load	35	0
2	Stockacher Aach; drainage from cultivated land	15–17	0
	Pleistocene		
3	Foreland of Alps; varved silty clays	30–35	0
2	Foreland of Alps; boulder clays	30–35	0
	Tertiary		
4	Upper Rhine Valley; mudstones, lacustrine (Neogene)	6–18	<5
4	Upper Rhine Valley; mudstones, lacustrine "Obere Pechelbronner Schichten" (Oligocene)	30–33	<5
3	Upper Rhine Valley; mudstones, brackish "Untere Pechelbronner Schichten" (Oligocene)	35	10–25
3	Upper Rhine Valley; mudstones, marine "Fischschiefer" (Oligocene)	30–35	30–35
	Upper Permian		
3	North Germany, Zechstein deposits; salt clays (evaporites)	35	>35
	Lower Permian		
10	Saar-Nahe region, Continental Permian Basin; reddish clayey siltstones	35	0
	Upper Carboniferous		
10	Ruhr; dark claystones overlying coal seam Plasshofsbank †	35	0–35
2	Ruhr; dark claystones from brackish environment	28–35	10–25
5	Ruhr; dark claystones from marine environment	28–35	>30

* Source and description. † Sampled at 1-cm intervals from top of coal seam. Environment changes from nonmarine (coal/claystone interface) to fully marine (10 cm above coal).